Scaffold-free trachea regeneration by tissue engineering with bio-three-dimensional printing

Daisuke Taniguchi[1,2], Keitaro Matsumoto[1,2], Tomoshi Tsuchiya[1], Ryusuke Machino[1], Yosuke Takeoka[1,2], Abdelmotagaly Elgalad[1,2], Kiyofumi Gunge[1,2], Katsunori Takagi[1,2], Yasuaki Taura[1], Go Hatachi[1], Naoto Matsuo[1,2], Naoya Yamasaki[1,2], Koichi Nakayama[3], Takeshi Nagayasu[1,2]

[1]Department of Surgical Oncology, Nagasaki University Graduate School of Biomedical Science, Japan

[2]Medical-engineering Hybrid Professional Development Program, Nagasaki University, Japan

[3]Department of Regenerative Medicine and Biomedical Engineering Faculty of Medicine, Saga University, Saga, Japan

Address correspondence to:

Takeshi Nagayasu

Department of Surgical Oncology, Nagasaki University Graduate School of Biomedical Sciences, Nagasaki 852-8501, Japan

Phone: +81-95-819-7304; Fax: +81-95-819-7306

E-mail: nagayasu@nagasaki-u.ac.jp

Meeting presentation: This manuscript was submitted and accepted to the 31st EACTS Annual Meeting, 7–11 October 2017, in Vienna, Austria

Word count: Total, 4987 words

Abstract

Objectives: Most previously reported artificial airway organs still require scaffolds; however, such scaffolds exhibit several limitations. Alternatively, the use of an autologous artificial trachea without foreign materials and immunosuppressants may solve these issues and constitute a preferred tool. The rationale of the present study was to develop a new scaffold-free approach for an artificial trachea using bio-three-dimensional (bio-3D) printing technology. Here, we assessed circumferential tracheal replacement using scaffold-free trachea-like grafts generated from isolated cells in an inbred animal model.

Methods: Chondrocytes and mesenchymal stem cells were isolated from F344 rats. Rat lung microvessel endothelial cells were purchased. Our bio-3D printer generates spheroids consisting of several types of cells to create 3D structures. The bio-3D-printed artificial trachea from spheroids was matured in a bioreactor and transplanted into F344 rats as a tracheal graft under general anesthesia. The mechanical strength of the artificial trachea was measured, and histological and immunohistochemical examinations were performed.

Results: Trachea transplantation was performed in nine rats, which were followed up to 23 days postoperation. The average tensile strength of the artificial tracheas before transplantation was 526.3 ± 125.7 mN. The bio-3D-printed scaffold-free artificial trachea had sufficient strength to transplant into the trachea with silicone stents, which were used to prevent collapse of the artificial trachea and to support the graft until sufficient blood supply was obtained. Chondrogenesis and vasculogenesis were observed histologically.

Conclusions: The scaffold-free isogenic artificial tracheas produced by a bio-3D printer could be utilized as trachea grafts in rats.

Key words: bio-three-dimensional printing, trachea regeneration, tissue engineering, scaffold-free artificial trachea

Introduction

The trachea functions as a conduit for ventilation; clears secretions; warms, humidifies, and cleans air for the respiratory zone; and keeps the airway free of foreign material through coughing and intrinsic defense mechanisms (1). General limits for safe tracheal resection include half of the tracheal length in adults and one-third in small children (1, 2). Thus, safe and dependable techniques for tracheal replacement are being developed. To date, many approaches including regeneration with tissue engineering have been developed for tracheal reconstruction; however, no standard procedures for tracheal transplantation/regeneration, particularly circumferential replacement, have been established (1, 3-5). Tracheal reconstruction is complex and challenging owing to difficulties in achieving revascularization because of the anatomical features of segmental blood supply, risk of infection owing to continuous contact with the outer environment, and rejection (1, 5). Notably, during tracheal reconstruction, the tissues must withstand both positive pressure inside and negative pressure; thus, the tissue must show sufficient strength.

Currently, most artificial airway organs still require scaffolds to maintain airway strength and stiffness (1, 3, 4, 6-9). However, scaffolds for artificial organs have some limitations, such as risk of infection, irritation, reduced biocompatibility, and degradation over time (2, 10). Furthermore, immunosuppression, which constitutes a risk of infection and a contraindication in malignant diseases, is also a problem (5). To solve these issues, scaffold-free approaches have been developed using bio-three-dimensional (bio-3D) printing with spheroids composed of aggregated cells (11-13). In tissue engineering, approaches with spheroids are considered to be promising. This technique utilizes the adhesive nature of the cells (11, 12). Additionally, a novel method to create scaffold-free tubular tissue from spheroids using a bio-3D printer-based system (Regenova) has been developed to enable the generation of 3D cellular structures by placing spheroids in fine needle arrays according to pre-designed 3D data using a computer-controlled robotics system (13). This technology may permit the production of autologous 3D structures by isolating autologous cells, and may allow optimal tracheal transplantation and regeneration without the use of foreign

81 materials and immunosuppressants. Here, we aimed to assess circumferential tracheal
82 replacement using artificial tracheas made via bio-3D printing from isolated primary cells,
83 such as chondrocytes and mesenchymal stem cells (MSCs), in inbred animals. We
84 examined the biological features of the bio-3D-printed artificial tracheas before and after
85 transplantation.
86

Materials and Methods

Animal care

This study was performed in strict accordance with the recommendations in the Guide for the Care and Use of Laboratory Animals of the National Institutes of Health. The study protocol was approved by the Institutional Animal Care and Use Committee of Nagasaki University (approval number 1708171402).

Cell isolation and culture

We used three-week-old male F344 rats (body weight: 50–70 g; Charles River Laboratories, Yokohama, Japan) to isolate cells. For MSC isolation, bone marrow cells were collected from animals sacrificed by cervical dislocation. The femurs were detached from the hind limbs and the muscles were removed. Bone marrow cells were isolated by flushing the femoral cavity with phosphate-buffered saline (PBS, Wako, Osaka, Japan) and culturing the obtained cells in Dulbecco's modified Eagle's medium (DMEM; Gibco, Gaithersburg, MD, USA) with heat-inactivated fetal bovine serum (FBS; Gibco) and 1% penicillin (100 IU/mL)/streptomycin (100 μg/mL; Gibco)/amphotericin B (0.25 μg/mL; Sigma-Aldrich, St. Louis, MO, USA) (14, 15). The isolated cells were evaluated by flow cytometry to determine CD29, CD31, CD34, CD44H, CD45, CD73, and CD90 expression using fluorescein isothiocyanate- or phycoerythrin-conjugated antibodies (BD Biosciences, San Jose, CA, USA). Cells were trypsinized, washed twice in PBS, incubated for 15 minutes at room temperature, and then washed twice. Samples were analyzed using a FACS Canto II (BD Biosciences). Most cells were positive for CD29, CD44H, CD73, and CD90 and negative for CD31, CD34, and CD45 (see Supplementary Figure).

For chondrocyte isolation, rib cartilage was harvested, and surrounding connective tissues were detached before being cut into smaller pieces. Chondrocytes were then isolated by enzymatic digestion. Briefly, cartilage specimens were minced and washed three times in PBS, and chondrocytes were isolated with 0.25% trypsin (Wako) in sterile saline followed by 0.25% collagenase type II (Gibco) in DMEM (16, 17).

Rat lung microvessel endothelial cells (RLMVECs; VEC Technologies Inc., Rensselaer, NY, USA) were purchased and cultured in endothelial cell growth medium (EGM) with growth supplement (Lonza, Inc., Warkersiville, MD, USA).

Isolated and purchased cells were cultured on 150-mm tissue culture dishes (TPP, Trasadingen, Switzerland) and maintained in a humidified cell culture incubator at 37°C with an atmosphere containing 5% CO_2. The cells were used within 3–9 passages.

Preparation of multicellular spheroids

Mixed cell suspensions (4.0×10^4 cells/spheroid) composed of chondrocytes from rib cartilage (70%), endothelial cells (20%), and MSCs (10%), were plated into ultra-low-attachment round-bottomed 96-U-well plates (Sumitomo Bakelite, Tokyo, Japan) containing chondrocyte growth medium (CGM) with growth supplement (Lonza) and EGM at a 1:1 ratio. The assay conditions were empirically chosen according to a preliminary experiment. After 72 hours, the cells aggregated spontaneously to form cell balls termed spheroids owing to their adhesive nature (11). These spheroids were used as bio-3D printing materials.

Bio-3D printing to generate tubular artificial tracheas

We used the Regenova bio-3D printer (Cyfuse Biomedical K.K., Tokyo, Japan) to assemble multicellular spheroids within a scaffold-free tubular artificial trachea. According to the 3D design, the bio-3D printer placed spheroids in a 9 × 9 needle array in a printer (3.2 mm in length per side). The needle outer diameter was 0.17 mm, and the distance between each needle was 0.4 mm. Spheroids were aspirated by a robotically controlled 25-gauge nozzle from the 96-well plate and inserted into the needle array, which was made of multiple medical-grade stainless needles automatically under computer control. In total, 384 spheroids were used to generate a 3D tubular structure. After bio-3D printing, the printed artificial trachea was matured inside the bioreactor with perfusion of medium (Figure 1).

The system was perfused with CGM and EGM media at 200 mL/h in bioreactor in a humidified cell culture incubator at 37°C with 5% CO_2. At seven days after spheroid placement onto the needle array, the needle array was removed and the printed artificial trachea was transferred to a 16-gauge plastic catheter (Terumo, Tokyo, Japan). The artificial trachea configuration was retained after removal from the needle array owing to inter-spheroid fusion. The duration prior to trachea transplantation was 28 days based on the results of our preliminary experiment and consideration of the most appropriate and longest permissible duration before surgery for clinical application (Figure 1).

Mechanical assessment

The tensile strength of three artificial tracheas (artificial trachea group) and three rings of the trachea from 3- (3-week rat trachea group) and 8-week-old rats (8-week rat trachea group) were measured to determine uniaxial tension using a Tissue Puller (DMT, Ann Arbor, MI, USA). Small stainless pins served as grips for individual samples. The samples were pulled in tension to failure at a rate of 50 μm/s. This test calculated the force at failure, as the maximum load that the artificial trachea/native trachea could withstand.

Surgical technique and follow up

Male (8–11-weeks old) F344 rats (200–260 g body weight; Charles River Laboratories) were used as recipients in this study. The rats were anesthetized using isoflurane (4%); anesthesia was maintained with isoflurane (2%). Spontaneous ventilation was maintained during the surgery. The cervical trachea was exposed through a cervical incision. Three rings of tracheal cartilage segments were resected and replaced with the scaffold-free bio-3D printed artificial trachea supported by a silicone stent (1.5 mm internal diameter; Kenis, Osaka, Japan). Proximal and distal end-to-end anastomoses were made with 8-0 polypropylene separate stitch sutures (Prolene; Ethicon Inc., Johnson & Johnson, Somerville, NJ, USA) microscopically. Stents were fixed to the trachea using an additional stitch. After achieving stable respiration, the cervical incision was closed.

Postoperatively, all recipient rats were observed for 1 to 2 hours before being returned to their individual cages. They received standard feed and water. To minimize the airway mucous output, atropine (0.05 mg/kg) was administered twice per day until sacrifice. No immunosuppressive therapy was administered. The follow-up period was 23 days postoperation. We did not remove the silicone stent in this study.

Histological and immunohistochemical examination

We sacrificed six animals at 1, 6, 8, 9, 11, and 23 days after transplantation for histological assessment (one rat each day). Animals were sacrificed on Day 11 and Day 23 to limit suffering owing to wheezing. Histological and immunohistochemical examinations were performed in spheroids, artificial tracheas before transplantation, and grafts after transplantation. All samples were fixed with 10% neutral buffered formalin (Japan Tanner Corporation, Osaka, Japan), embedded in paraffin, and sectioned (5-μm thickness); the mounted tissue sections were deparaffinized and rehydrated before analysis. Morphological analyses of the distribution of cartilage tissue, red blood cells, fibrosis, and connective tissue of the spheroids, artificial tracheas, and transplanted grafts were performed on sections stained with hematoxylin-eosin (HE) using light microscopy. Alcian blue (pH 1.0; Muto Pure Chemicals, Tokyo, Japan) staining was performed to assess glycosaminoglycans (GAG) as a main component of cartilage tissue. Immunohistochemistry was performed with primary antibodies (anti-collagen II [rabbit polyclonal; 600-401-104-408; Rockland, Limerick, PA, USA], anti-CD31 [rabbit polyclonal; bs-195R; Bioss, Boston, MA, USA], and anti-pan cytokeratin [mouse monoclonal; ab7753; Abcam, Cambridge, UK). Anti-collagen II, anti-CD31, and anti-pan cytokeratin were selected to assess cartilage tissue and chondrogenesis, endothelial cell distribution and vasculogenesis, and epithelialization, respectively.

GAG assays

Total GAGs of artificial tracheas (artificial trachea group) and native rat tracheas (3- and 8-week rat trachea groups), and transplanted grafts resected on Day 7 (graft after

transplantation group) were measured by BLYSCAN assays (Biocolor, Belfast, Northern Ireland). For the assessment on Day 7, three rats were sacrificed, and tracheal grafts were trimmed of surrounding connective tissues microscopically. We used PicoGreen reagent (Molecular Probes, Eugene, OR, USA) to quantify double-stranded DNA for normalization of the amount of GAGs.

Statistical analysis

Data are reported as the mean ± standard deviation. All statistical analyses were performed using JMP Pro software (version 11.2.0; SAS Institute, Inc., Cary, NC, USA). Comparisons were performed using analysis of variance with Tukey's honestly significant difference test. Results with $p < 0.05$ were considered statistically significant.

Results

Gross morphological assessment of artificial tracheas

Artificial tracheas were assessed after 28 days of total maturation following bio-3D printing. The bio-3D-printed artificial tracheas were whitish-yellow in color (Figure 2-A). The wall length and thickness were 5.52 ± 0.14 and 0.53 ± 0.03 mm, respectively. The artificial tracheas were easy to handle with surgical forceps.

Mechanical properties

The average tensile strength was 526.3 ± 125.7, 387.3 ± 120.0, and 1060.3 ± 91.1 mN in the artificial trachea, 3-week rat trachea, and 8-week rat trachea groups, respectively. The artificial trachea and 8-week rat trachea groups differed significantly, whereas no significant difference existed between the artificial trachea and 3-week rat trachea groups (Figure 2-B).

Macroscopic assessment after trachea transplantation

Tracheal transplantation was conducted without any complications (Figure 3-A, B). The length of the bio-3D-printed artificial trachea as the graft for tracheal transplantation was 4.82 ± 0.81 mm. After sacrifice and resection of the transplanted trachea, all tracheal grafts maintained shape and stiffness. Some connective tissue with microvessels surrounding the tracheal grafts was observed (Figure 3-C, D). As a postoperative complication, wheezing owing to retention of tracheal secretions was observed in two rats.

GAG assays

GAG content normalized to DNA content was 124.7 ± 65.7, 70.0 ± 1.5, 199.1 ± 15.1, and 222.7 ± 13.0 μg/μg in the artificial trachea, graft after transplantation, 3-week rat trachea, and 8-week rat trachea groups, respectively. The GAG content was significantly lower in the graft after transplantation group than in the 3- and 8-week rat trachea groups; no significant

differences were observed between the artificial trachea and graft after transplantation groups or between the artificial trachea and rat trachea groups (Figure 4).

Histological assessment of artificial tracheas and grafts

Alcian blue staining for GAG production showed slight blue staining in spheroids, and GAG deposits were found in the bio-3D-printed artificial tracheas after the maturation period; GAGs persisted over 10 days (Figure 5).

Immunohistochemistry showed slight collagen II expression in spheroids; however, collagen II was observed in the artificial tracheas after maturation and maintained after tracheal transplantation (Figure 5). Some small capillary-like tube formations consisting of CD31-positive cells were observed in the artificial tracheas and increased in number over time (Figure 5). HE staining showed red blood cells inside the capillary-like tube formations from Day 8 (Figure 5, 6-A-D). Cartilage tissue and the size and number of capillary-like tube formations further increased in the transplanted graft on Day 23 (Figure 5, 6-A-D). Epithelialization started from Day 8 and proceeded until Day 23, although total epithelialization was not obtained by Day 23 (Figure 6-E, F). Small amounts of inappropriate granulosis were observed from Day 8.

Discussion

The trachea is a complex organ containing multiple tissue types to provide the organ with its specific function (3). Most trials for tracheal regeneration require scaffolds to maintain airway strength and stiffness (1, 3, 5, 7-9, 18, 19). However, no method is yet widely applicable for clinical treatment, and the use of scaffolds for artificial organs has some limitations (2, 10). Thus, tracheal reconstruction using a scaffold-free artificial trachea prepared using autologous cells would be preferred. Here, we achieved orthotopic circumferential trachea transplantation without immunosuppression using scaffold-free artificial tracheas generated by bio-3D printing in an inbred animal model. The artificial trachea constructed using various types of isolated cells matured *in situ* and was functional for several weeks after transplantation without requiring immunosuppressants.

Production of scaffold-free structures is somewhat difficult owing to the lack of structural integrity (4). In this study, we utilized a bio-3D printer to produce scaffold-free artificial tracheas. This technique can facilitate creation of small-caliber vascular prosthesis and peripheral nerve regeneration (11, 20). We confirmed the existence of cartilage tissue in the scaffold-free artificial tracheas and found that incubation for 4 weeks permitted maturation in terms of chondrogenesis and vasculogenesis from the spheroids, as shown by histological analysis. Additionally, the bio-3D-printed scaffold-free artificial trachea showed sufficient mechanical strength for transplantation into the trachea with silicone stent support.

Silicone stents were used to support the inner lumen during tracheal transplantation because the tensile strength was lower than that of native adult rat trachea and it was necessary to prevent collapse in the acute phase after tracheal transplantation. Additionally, the stent itself was soft and sufficiently elastic to remain inside the tracheal lumen without injury to the inner lumen or disruption of epithelial cell extension. A certain amount of time was required to obtain stable transplanted grafts through revascularization and growth of surrounding connective tissue because support from the surrounding tissue is necessary for appropriate vasculogenesis. Additionally, the grafts tended to be less patent, as shown by the thick secretions, coughing, and inability to aspirate in the small animal model (18),

necessitating atropine administration to enhance airway clearance and decrease respiratory secretion. Some studies have reported tracheal regeneration without stents in animal models, including reports describing circumferential replacement by tissue-engineered tracheal grafts with scaffolds (2, 5) and partial trachea wall replacement (21). In our study, inappropriate granulation was observed as a negative effect of the stents, potentially because of both the lack of luminal surface epithelialization and the stent insertion. Epithelial regeneration plays an essential role in the patency of tracheal grafts, preventing fibroblast proliferation (5, 22, 23). Our scaffold-free approach showed maturation potential, even after transplantation, as native epithelium extension was found on Day 8 and was expected to completely cover the artificial trachea surface. Removal of the stent for long-term follow up may be needed; investigations are ongoing in our laboratory. In addition, bronchoscopic interventions, such as silicone stent removal and ablation of granulation, can be more easily performed in larger animals or humans. We believe this strategy may have practical clinical application in the future, and our findings demonstrating short-term survival in rats and bio-3D printed artificial trachea maturation after transplantation provide a basis for further study.

We assessed the presence of GAG and collagen II as main components of cartilage (3, 24). Our findings show that cartilaginous tissue was formed during the maturation period following bio-3D printing and maintained after transplantation, although the distribution differed from that of the normal native tissue. GAG and collagen II were present, as demonstrated by cartilaginous tissue formation (Alcian blue staining) and immunohistochemical staining for collagen II. Additionally, cartilaginous tissue was maintained for over 10 days after transplantation, with the highest amount of cartilaginous tissue observed on Day 23. GAG assays indicated no significant differences in the GAG amount between artificial tracheas and rat trachea samples; the GAG amount tended to decrease after transplantation, although this finding was not significant. As chondrogenesis is related to vasculogenesis, the GAG amount increased after Day 8, consistent with histological findings. The GAG amount in the artificial trachea may be related to material mechanical strength. To assess the minimum airway tensile strength, we evaluated tracheal

tissues in rats at 3 and 8 weeks of age; although no significant differences were observed, the force at failure for artificial tracheas tended to be higher than that of 3-week-old rat tracheas.

Airway reconstruction is challenging owing to tissue anatomical features including segmental blood supply with a network of small vessels, which can result in ischemia after transplantation (1, 6). Moreover, the lack of an individualized vascular pedicle, which impedes immediate revascularization (19), remains a challenge in tracheal replacement. In chondrocyte, endothelial cell, and MSC co-cultures, both osteogenesis and vasculogenesis are enhanced (25), and MSCs facilitate engineering of long-lasting functional vasculature when co-implanted with endothelial cells (26). To obtain immediate revascularization, we utilized endothelial cells and MSCs as the cell source for scaffold-free artificial tracheas. Capillary-like tube formation was observed in bio-3D printed artificial tracheas before tracheal transplantation, the numbers of which increased after transplantation. Furthermore, red blood cells inside the formed tubes were observed from Day 8, also subsequently increasing. Some amount of connective tissue with microvessels surrounding the tracheal graft was observed in the macroscopic findings. These results showed that appropriate vasculogenesis could be obtained in scaffold-free trachea transplantation with our bio-3D printing technique.

MSCs are an attractive, clinically relevant cell source for neocartilage formation (3) and can be harvested from patient bone marrow with a minimally invasive procedure. Furthermore, MSCs can be easily expanded in vitro to obtain the needed cell numbers and constitute an ideal cell source for cell transplantation and tissue engineering (3, 18). MSCs can also have trophic effects on chondrocyte proliferation and matrix deposition (27) and are important for vasculogenesis, as demonstrated in this study. Although we did not investigate MSC differentiation after transplantation, we assumed that our use of MSCs was appropriate and effective, consistent with previous reports.

Although immunosuppression was not performed, acute rejection was not observed in this study. Moreover, because we did not use scaffolds, the foreign body reaction was

lower than that in scaffold-based approaches. Immunosuppression must be avoided in airway regeneration owing to the high risk of infection and its contraindication in malignancies. Trachea regeneration can be utilized for bronchus replacement (7, 8), in lung cancer surgery requiring bronchoplasty, as well as in airway regeneration in the future.

Additional studies are needed to confirm the potential applications of this technology, including long-term follow-up for analysis of transplanted tracheal segment growth, removal of the stent after a certain period, and observation of epithelialization and revascularization with support of native tissue. In addition, experiments in large animal models will be required for clinical application. These investigations are ongoing in our laboratory, and we are pursuing further clinical studies of this technology.

Conclusion

This work demonstrated our initial experience of tracheal tissue engineering with bio-3D printing technology using a scaffold-free approach. The artificial tracheas produced by the bio-3D printer with isolated rat cells could be transplanted via isogenic trachea transplantation. This technology may have applications in tracheal regeneration.

Acknowledgments

We thank Kazuo Yamamoto and Hideki Muto (Biomedical Research Support Center, Nagasaki University School of Medicine) for their excellent technical assistance in flow cytometry.

Funding statement

This work was supported by a Japan Society for the Promotion of Science KAKENHI Grant-in-Aid for Scientific Research (C) (grant no. JP26462147).

Conflict of Interest: none declared.

Figure Legends

Figure 1. Scheme and process for artificial trachea generation.

First, cells such as chondrocytes and mesenchymal stem cells are isolated and cultured. Then, we prepared multicellular spheroids using the cells and performed bio-3D printing. The artificial tracheas were matured in a bioreactor for an appropriate duration. Finally, isogenic trachea transplantation of the artificial trachea was performed.

Figure 2. Macroscopic and mechanical assessment of the artificial tracheas.

A. Gross macroscopic pictures of bio-3D printed artificial tracheas before transplantation. Scale bar = 2 mm. B. Force at failure of artificial tracheas and native tracheas. Error bars indicate standard deviation of the mean. *, $p < 0.05$.

Figure 3. Tracheal transplantation and macroscopic findings after transplantation.

A. Tracheal defects after resection of the trachea during the operation. B. Photograph of the surgical field after transplantation of the graft. C. Day 7 postoperation. Some connective tissue with microvessels surrounding the tracheal graft was observed. Scale bar = 2 mm. D. Day 7 postoperation and after removal of the stitches and stent inside the graft (arrows: junction between the graft and trachea). Scale bar = 2 mm.

Figure 4. GAG assays.

Data showing GAG content in the various groups. Transplanted grafts extracted on Day 7 in the graft after transplantation group. Error bars indicate the standard deviation of the mean. *, $p < 0.05$. GAG: glycosaminoglycan.

Figure 5. Histological findings of the spheroids, artificial tracheas, and transplanted grafts.

A–F: HE staining, G–L: immunohistochemical staining with anti-CD31 antibodies, M–R: Alcian blue staining, S–X: immunohistochemical staining with anti-collagen II antibodies.

Spheroids: A, G, M, and S. Bio-3D printed artificial tracheas after maturation: B, H, N, and T. Day 1: C, I, O, and U. Day 8: D, J, P, and V. Day 11: E, K, Q, and W. Day 23: F, L, R, and X. Cartilage tissue can be observed in artificial tracheas after maturation and maintained over 10 days (asterisk). Capillary-like tubes consisting of CD31-positive cells (arrow) can be seen in artificial tracheas after maturation. Red blood cells are observed from Day 8 in the capillary-like tube formations (arrowhead). Scale bar = 100 μm. HE: hematoxylin-eosin.

Figure 6. Vascularization and epithelialization of the graft on Day 8 and Day 23.

A, C, E: Day 8. B, D, F: Day 23. A, B: HE staining, Scale bar = 50 μm. C, D: Immunohistochemical staining with anti-CD31 antibodies, Scale bar = 50 μm. HE staining shows red blood cells inside the capillary-like tube formations consisting of CD31-positive cells (arrow-heads) on Day 8. The size and number of capillary-like tube formations increased on Day 23. E, F: Immunohistochemical staining with anti-pan-cytokeratin antibodies. Epithelialization started from Day 8 (arrow: junction between graft and native trachea) and extended on Day 23 (EE: extended airway epithelial cells). Scale bar = 100 μm. HE: hematoxylin-eosin.

Figure 1

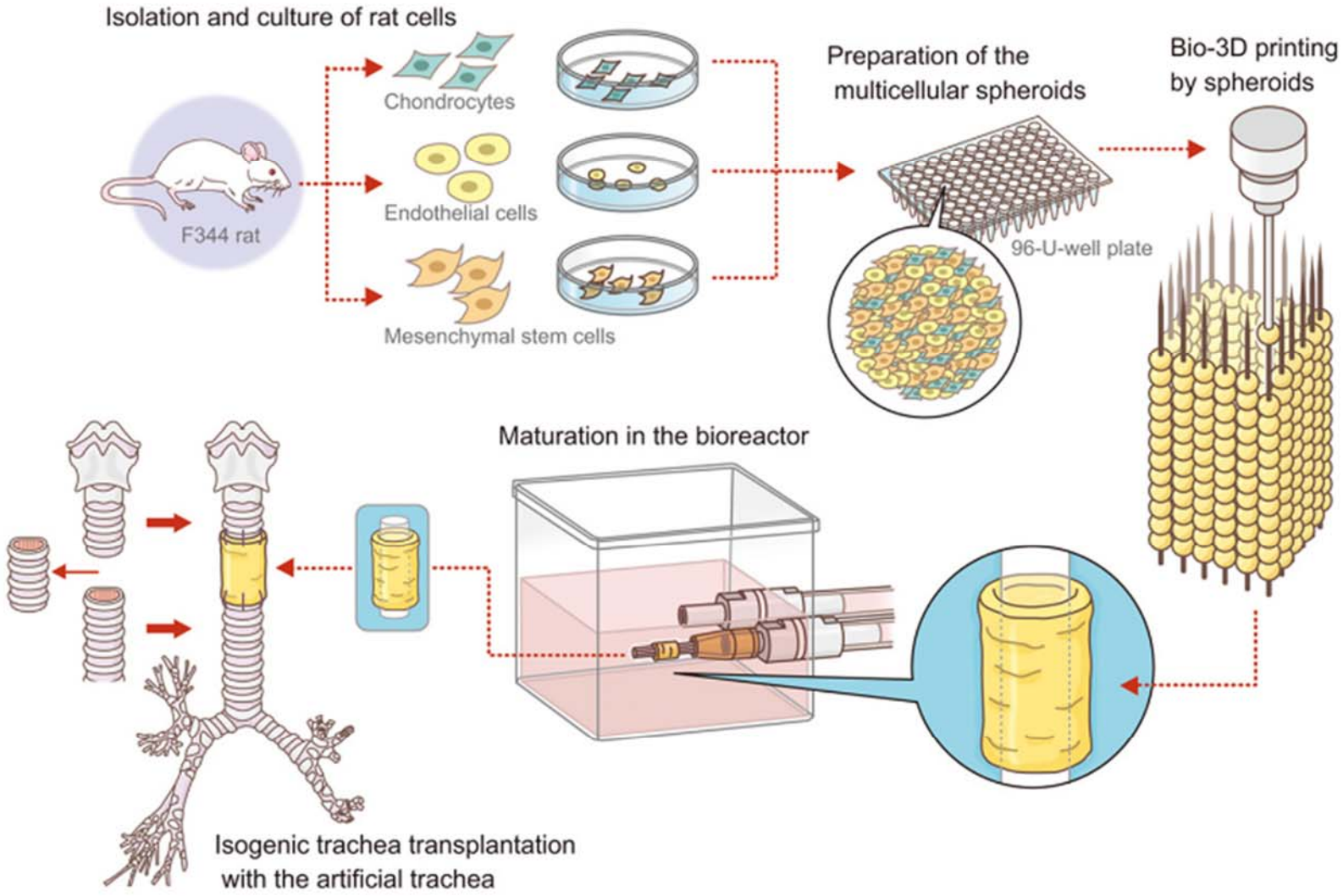
Isolation and culture of rat cells
F344 rat
Chondrocytes
Endothelial cells
Mesenchymal stem cells
Preparation of the multicellular spheroids
96-U-well plate
Bio-3D printing by spheroids
Maturation in the bioreactor
Isogenic trachea transplantation with the artificial trachea

414 **Figure 2**

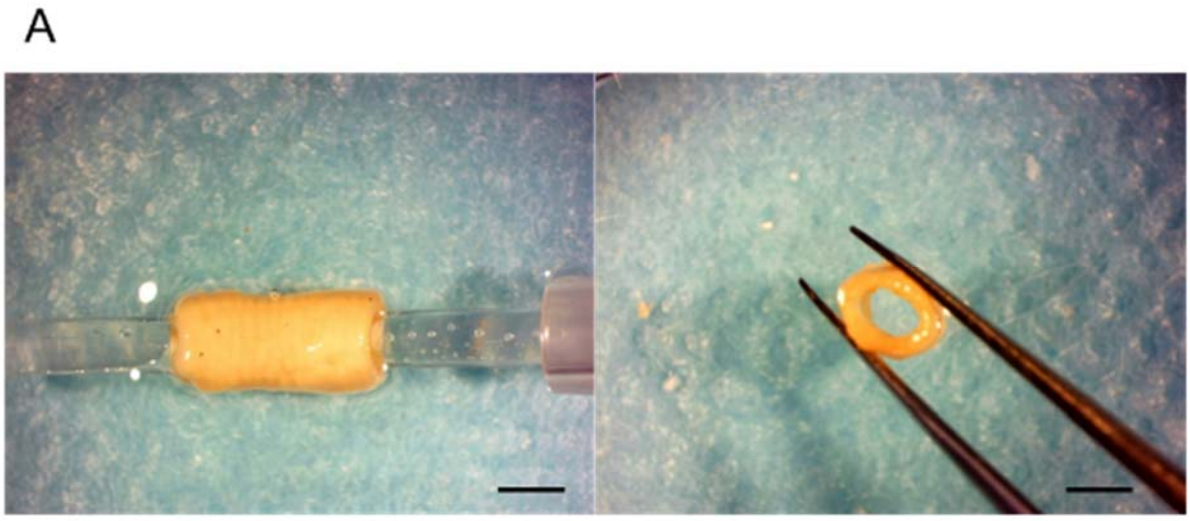

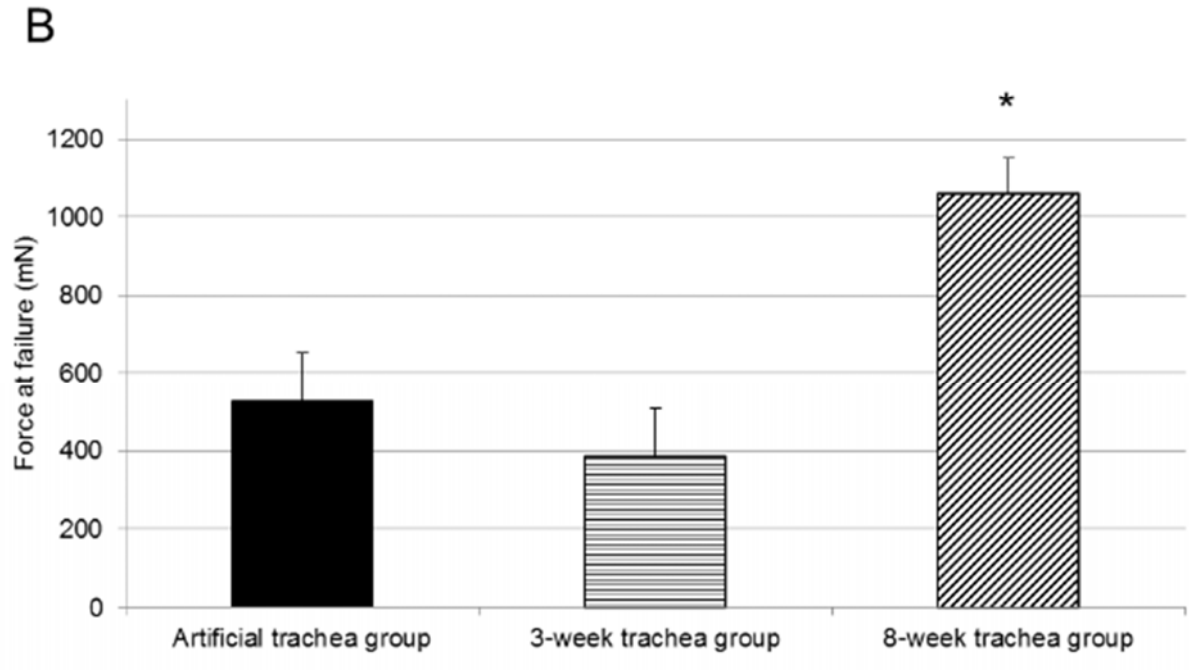

415
416

417 **Figure 3**

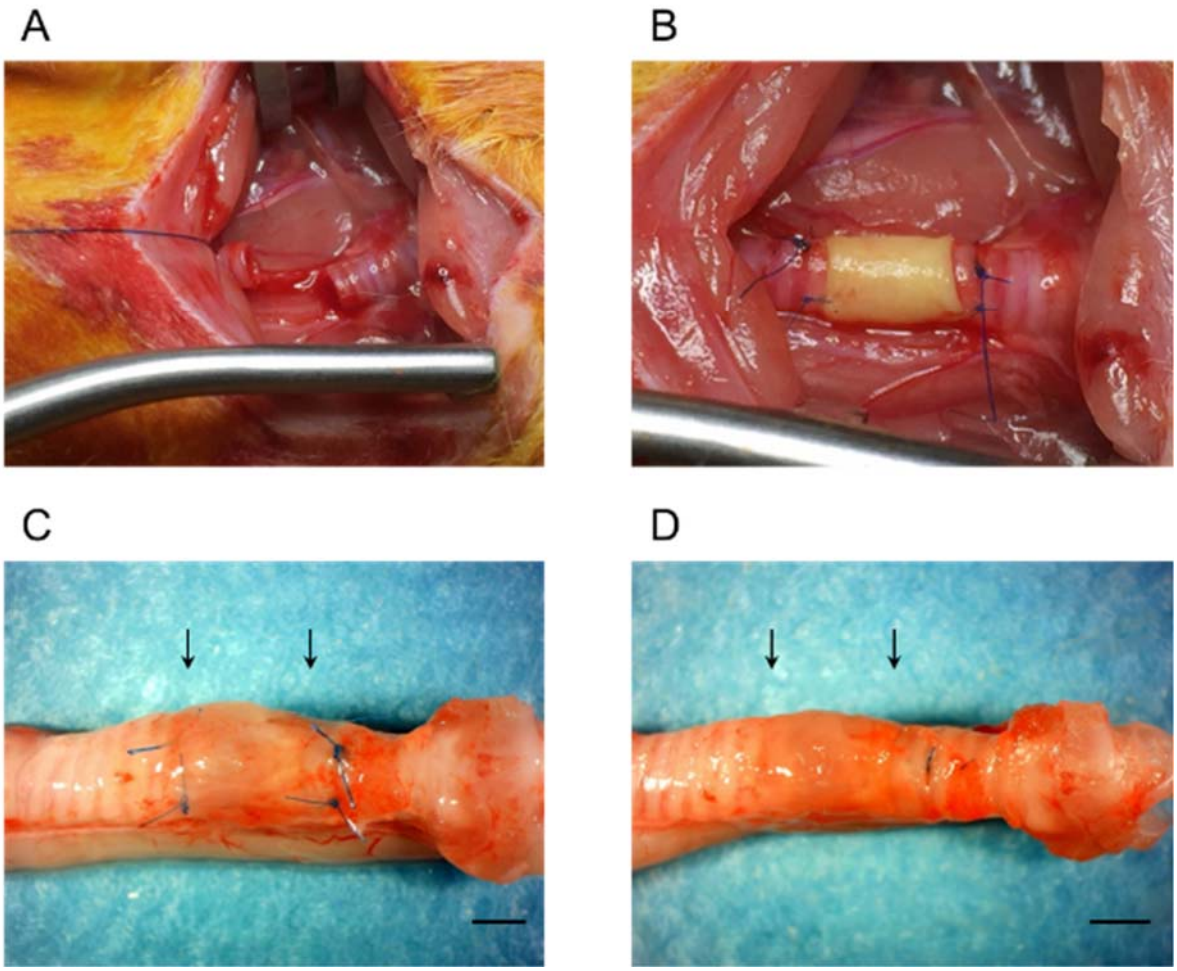

418

Figure 4

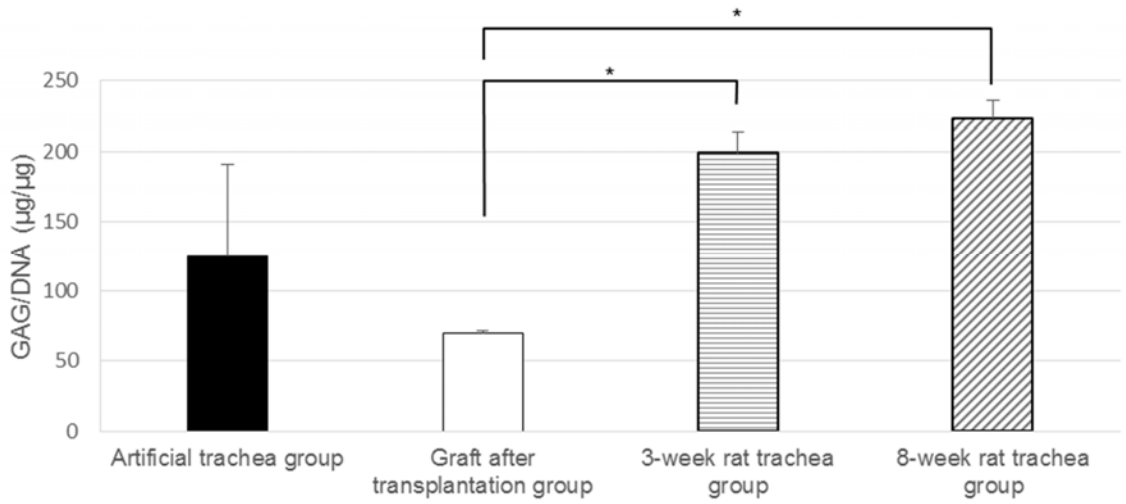
*
*
250
200
150
100
50
0
GAG/DNA (μg/μg)
Artificial trachea group
Graft after transplantation group
3-week rat trachea group
8-week rat trachea group

Figure 5

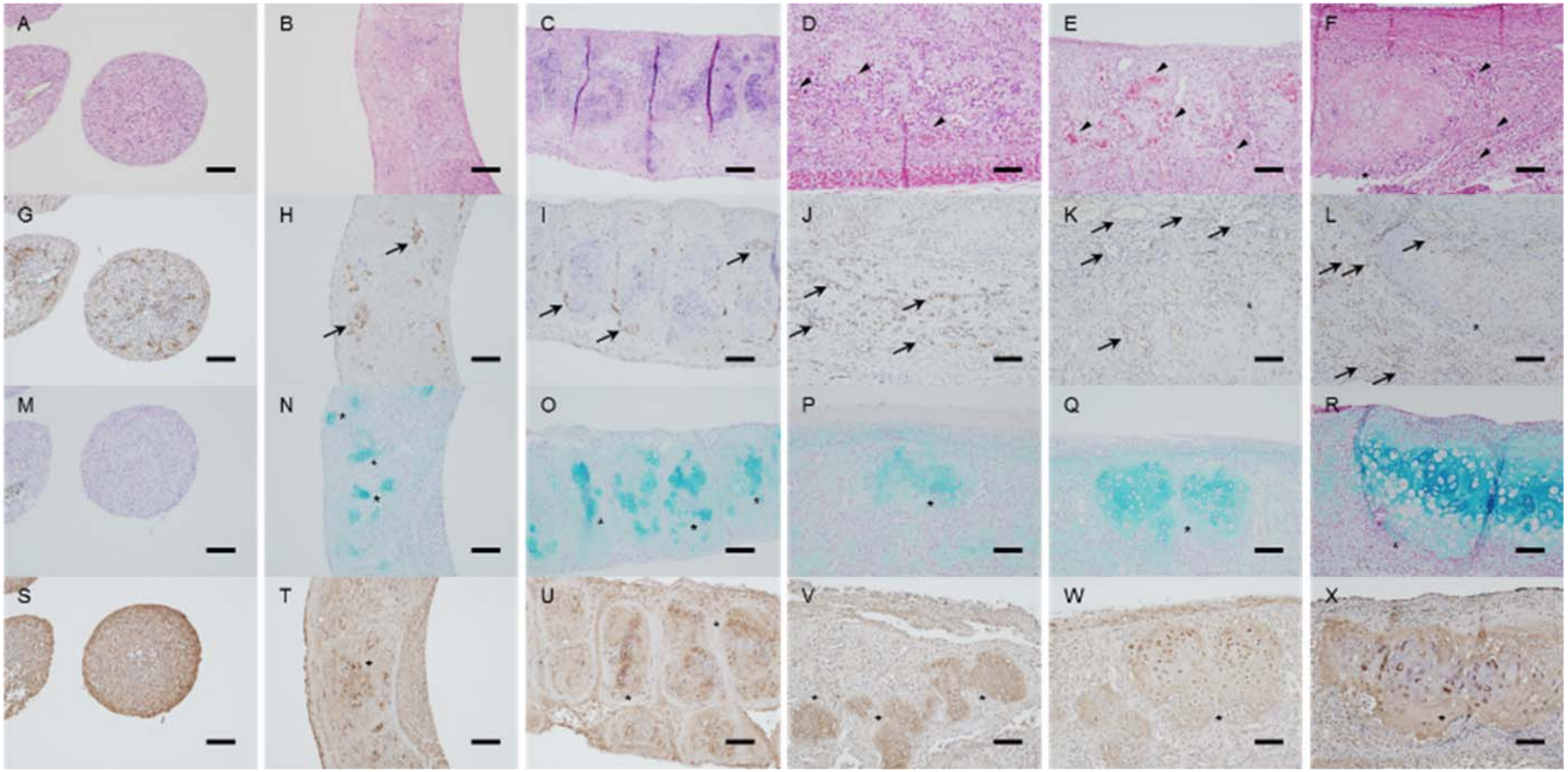

Figure 6

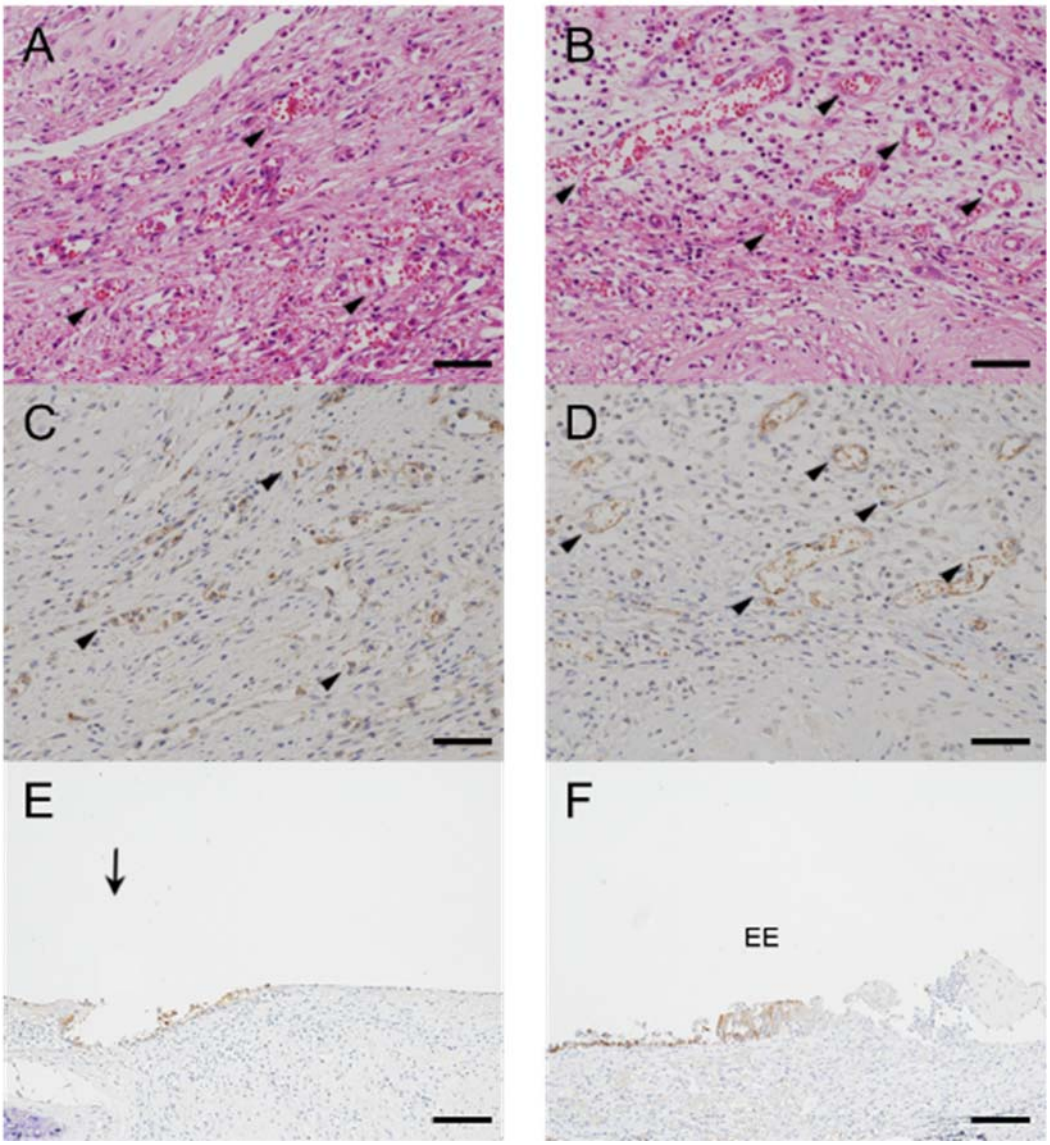

References

1. Haykal S, Salna M, Waddell TK, Hofer SO. Advances in tracheal reconstruction. Plast Reconst Sur Glob Open 2014;2:e178

2. Jungebluth P, Haag JC, Sjöqvist S, Gustafsson Y, Beltrán Rodríguez A, Del Gaudio C, *et al*. Tracheal tissue engineering in rats. Nat Protoc 2014;9:2164–79.

3. Dikina AD, Strobel HA, Lai BP, Rolle MW. Engineered cartilaginous tubes for tracheal tissue replacement via self-assembly and fusion of human mesenchymal stem cell constructs. Biomaterials 2015;52:452–62.

4. Jungebluth P, Macchiarini P. Airway transplantation. Thorac Surg Clin 2014;24:97–106.

5. Hysi I, Kipnis E, Fayoux P, Copin MC, Zawadzki C, Jashari R, *et al*. Successful orthotopic transplantation of short tracheal segments without immunosuppressive therapy. Eur J Cardiothorac Surg 2015;47:e54–61.

6. Delaere P, Vranckx J, Verlenden G, De Leyn P, Van Raemdonck D; Leuven Tracheal Transplant Group. Tracheal allotransplantation after withdrawal of immunosuppressive therapy. N Eng J Med 2010;362:138–45.

7. Gonfiotti A, Jaus MO, Barale D, Baiguera S, Comin C, Lavorini F, *et al*. The first tissue-engineered airway transplantation: 5-year follow-up results. Lancet 2014;383:238–44.

8. Tan Q, Liu R, Chen X, Wu J, Pan Y, Lu S, *et al*. Clinic application of tissue engineered bronchus for lung cancer treatment. J Thorac Dis 2017;9:22–29.

9. Hamilton NJ, Kanani M, Roebuck DJ, Hewitt RJ, Cetto R, Culme-Seymour EJ, *et al*. Tissue-engineered tracheal replacement in a child: a 4-year follow-up study. Am J Transplant 2015;15:2750–7.

10. Kelm JM, Lober V, Snederker JG, Schmidt D, Broggini-Tenzer A, Weisstanner M, *et al*. A novel concept for scaffold-free vessel tissue engineering: self-assembly of microtissue building blocks. J Biotechnol 2010;148:46–55.

11. Itoh M, Nakayama K, Noguchi R, Kamohara K, Furukawa K, Uchihashi K, *et al*. Scaffold-free tubular tissues created by a Bio-3D printer undergo remodeling and endothelialization when implanted in rat aortae. PLoS One 2015;10:e0136681.

12. Fennema E, Rivron N, Roukema J, Bitterswijk CV, Boer J. Spheroid culture as a tool for creating 3D complex tissues. Trends Biotechnol 2013;31:108–15.

13. Nakayama K. In bitro biofabrication of tissue and organs. Biofabrication 2013;1–21.

14. Tsubokawa T, Yagi K, Nakanishi C, Zuka M, Nohara A, Ino H, *et al*. Impact of anti-apoptotic and anti-oxidative effects of bone marrow mesenchymal stem cells with transient overexpression of heme oxygenase-1 on myocardial ischemia. Am J Physiol Heart Circ Physiol 2010;298:H1320–9.

15. Nagaya N, Fujii T, Iwase T, Ohgushi H, Itoh T, Uematsu M, *et al*. Intravenous administration of mesenchymal stem cells improves cardiac function in rats with acute myocardial infarction through angiogenesis and myogenesis. Am J Physiol Heart Circ Physiol 2004;287:H2670–6.

16. Kawasaki K, Ochi M, Uchio Y, Adachi N, Matsusaki M. Hyaluronic acid enhances proliferation and chondroitin sulfate synthesis in cultured chondrocytes embedded in collagen gels. J Cell Physiol 1999;179:142–8.

17. Yasui N, Osawa S, Ochi T, Nakashima H, Ono K. Primary culture of chondrocytes embedded in collagen gels. Exp Cell Biol 1982;50:92–100.

18. Seguin A, Baccari S, Holder-Espinasse M, Bruneval P, Carpentier A, Taylor DA, *et al*. Tracheal regeneration: evidence of bone marrow mesenchymal stem cell involvement. J Thorac Cardiovasc Surg 2013;145:1297–304.

19. Hysi I, Wurtz A, Zawadzki C, Kipnis E, Jashari R, Hubert T, *et al*. Immune tolerance of epithelium-denuded-cryopreserved tracheal allograft. Eur J Cardiothorac Surg 2014;45:e180–6.

20. Yurie H, Ikeguchi R, Aoyama T, Kaizawa Y, Tajino J, Ito A, *et al*. The efficacy of a scaffold-free Bio 3D conduit developed from human fibroblasts on peripheral nerve regeneration in a rat sciatic nerve model. PLoS One 2017;12:e0171448.

21. Yamashita M, Kanemaru S, Hirano S, Tamura Y, Umeda H, Ohno T, *et al*. A regenerative approach for partial tracheal defects, an in vivo canine model. Inflamm Regen 2007;27:570–4.

22. Ikonen TS, Brazelton TR, Berry GJ, Shorthouse RS, Morris RE. Epithelial re-growth is associated with inhibition of obliterative airway disease in orthotopic tracheal allografts in non-immunosuppressed rats. Transplantation 2000;70:857–63.

23. Go T, Jungebluth P, Baiguero S, Asnaghi A, Martorell J, Ostertag H, et al. Both epithelial cells and mesenchymal stem cell–derived chondrocytes contribute to the survival of tissue-engineered airway transplants in pigs. J Thorac Cardiovasc Surg. 2010;139:437–43.

24. Ayerst BI, Merry CLR, Day AJ. The good the bad and the ugly of glycosaminoglycans in tissue engineering applications. Pharmaceuticals (Basel) 2017;10:E54.

25. Freeman FE, Stevens HY, Owens P, Guldberg RE, McNamara LM. Osteogenic differentiation of mesenchymal stem cells by mimicking the cellular niche of the endochondral template. Tissue Eng Part A 2016;22:1176–90.

26. Au P, Tam J, Fukumur D, Jain RK. Bone marrow-derived mesenchymal stem cells facilitate engineering of long-lasting functional vasculature. Blood 2008;111:4551–8.

27. Wu L, Leijten JC, Georgi N, Post JN, van Blitterswijk CA, Karperien M. Trophic effects of mesenchymal stem cells increase chondrocyte proliferation and matrix formation. Tissue Eng Part A 2011;17:1425–36.